Title

Modeling the 3D Geometry of the Cortical Surface with Genetic Ancestry

Journal

Current Biology, 25(15)

ISSN

0960-9822

Authors

Fan, Chun Chieh
Bartsch, Hauke
Schork, Andrew J
et al.

Publication Date

2015-08-01

DOI

10.1016/j.cub.2015.06.006

Peer reviewed

Report

Current Biology

Modeling the 3D Geometry of the Cortical Surface with Genetic Ancestry

Graphical Abstract

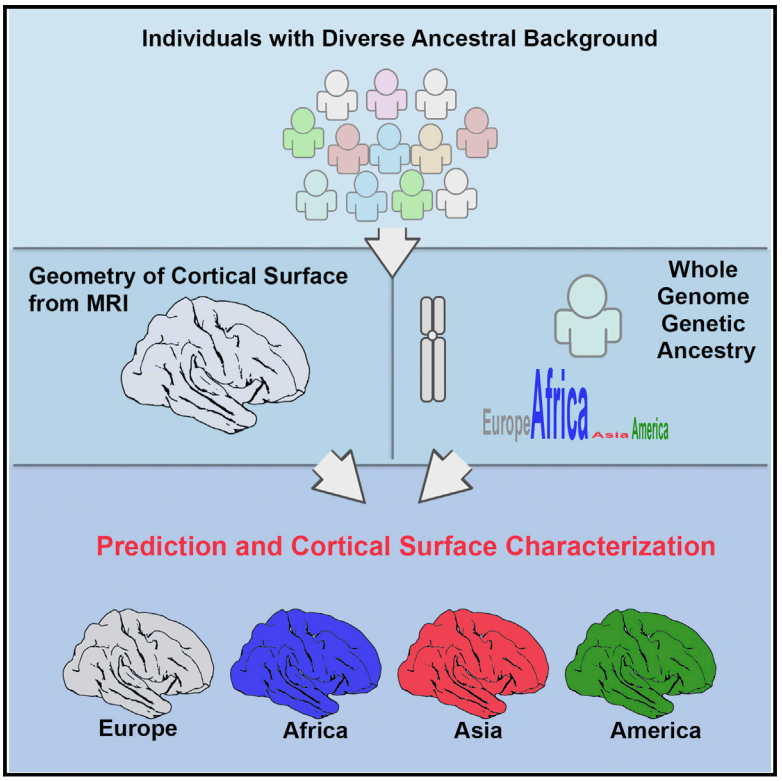

Highlights

- Geometry of the human cortical surface contains rich ancestral information
- The most informative features are regional patterns of cortical folding and gyrification
- This study provides insight on the influence of population structure on brain shape

Authors

Chun Chieh Fan, Hauke Bartsch, Andrew J. Schork, ..., Nicholas J. Schork, Terry L. Jernigan, Anders M. Dale

Correspondence

amdale@ucsd.edu

In Brief

Fan et al. show that human cortical surface robustly predicts an individual's genetic ancestry despite that populations have been shaped by waves of migrations and admixture events. For each continental ancestry, the regional patterns of cortical folding and gyrification are unique and complex.

Fan et al., 2015, Current Biology *25*, 1988–1992
August 3, 2015
http://dx.doi.org/10.1016/j.cub.2015.06.006

CellPress

CellPress

Current Biology
Report

Modeling the 3D Geometry of the Cortical Surface with Genetic Ancestry

Chun Chieh Fan,[1] Hauke Bartsch,[2] Andrew J. Schork,[1] Chi-Hua Chen,[3] Yunpeng Wang,[2,4,5] Min-Tzu Lo,[3] Timothy T. Brown,[2,5] Joshua M. Kuperman,[2,3] Donald J. Hagler, Jr.,[2,3] Nicholas J. Schork,[6] Terry L. Jernigan,[1,3,7,8] Anders M. Dale,[1,2,3,5,8,*] and the Pediatric Imaging, Neurocognition, and Genetics Study

[1]Department of Cognitive Science, University of California, San Diego, 9500 Gilman Drive, La Jolla, CA 92093, USA
[2]Multimodal Imaging Laboratory, University of California, San Diego School of Medicine, 9500 Gilman Drive, La Jolla, CA 92037, USA
[3]Department of Radiology, University of California, San Diego School of Medicine, 9500 Gilman Drive, La Jolla, CA 92037, USA
[4]Norwegian Centre for Mental Disorders Research (NORMENT), KG Jebsen Centre for Psychosis Research, Institute of Clinical Medicine, University of Oslo, 0424 Oslo, Norway
[5]Department of Neuroscience, University of California, San Diego School of Medicine, 9500 Gilman Drive, La Jolla, CA 92037, USA
[6]J. Craig Venter Institute, Capricorn Lane, La Jolla, CA 92037, USA
[7]Center for Human Development, University of California, San Diego, 9500 Gilman Drive, La Jolla, CA 92161, USA
[8]Department of Psychiatry, University of California, San Diego School of Medicine, 9500 Gilman Drive, La Jolla, CA 92037, USA
*Correspondence: amdale@ucsd.edu
http://dx.doi.org/10.1016/j.cub.2015.06.006

SUMMARY

Knowing how the human brain is shaped by migration and admixture is a critical step in studying human evolution [1, 2], as well as in preventing the bias of hidden population structure in brain research [3, 4]. Yet, the neuroanatomical differences engendered by population history are still poorly understood. Most of the inference relies on craniometric measurements, because morphology of the brain is presumed to be the neurocranium's main shaping force before bones are fused and ossified [5]. Although studies have shown that the shape variations of cranial bones are consistent with population history [6–8], it is unknown how much human ancestry information is retained by the human cortical surface. In our group's previous study, we found that area measures of cortical surface and total brain volumes of individuals of European descent in the United States correlate significantly with their ancestral geographic locations in Europe [9]. Here, we demonstrate that the three-dimensional geometry of cortical surface is highly predictive of individuals' genetic ancestry in West Africa, Europe, East Asia, and America, even though their genetic background has been shaped by multiple waves of migratory and admixture events. The geometry of the cortical surface contains richer information about ancestry than the areal variability of the cortical surface, independent of total brain volumes. Besides explaining more ancestry variance than other brain imaging measurements, the 3D geometry of the cortical surface further characterizes distinct regional patterns in the folding and gyrification of the human brain associated with each ancestral lineage.

RESULTS

The participants were recruited as part of the Pediatric Imaging, Neurocognition, and Genetics (PING) study. A detailed overview of the study can be found in previous publications (e.g., [3, 4, 10]), and research protocols and data are publicly available online [11]. Briefly, PING was a multisite project recruiting children and adolescents from ages 3 to 21 at ten sites in the United States. All participants were screened for history of major developmental, psychiatric, and neurological disorders; brain injury; and other medical conditions that affect development. Participants then received neurodevelopmental assessments, standardized multimodal neuroimaging, and genome-wide genotyping. The overall PING sample consisted of 1,493 participants; 1,152 individuals remained after quality control of the genotyping and neuroimaging data (for quality-control processes and demographics of the participants, see Supplemental Experimental Procedures and Table S1). We focused our analyses on 562 individuals older than 12 years (289 males, mean age 16.6 years, standard deviation 2.6 years). Considering that the morphological features of cortical surface change little after age 12 [10], this stratified approach further reduced the residual confounds of developmental effects.

The proportions of genetic ancestry were estimated using principal component (PC) analysis with whole-genome SNP reference panels for ancestry [12–14]. Four continental populations were used as ancestral references: West Africa (YRI, Yoruba in Ibadan), Europe (CEU, Utah residents with Northern and Western European ancestry), East Asia (EA), and America (NA, Native American). The metrics for summarizing genetic ancestry in each ancestral component were standardized as proportions ranging from 0% to 100%. These proportions represent how genetically similar an individual is to the reference population [14].

Morphological Prediction for Genetic Ancestry

We first tested whether the surface geometry of the cerebral cortex predicted the proportion of genetic ancestry among participants. To characterize variation in the geometry, we reconstructed

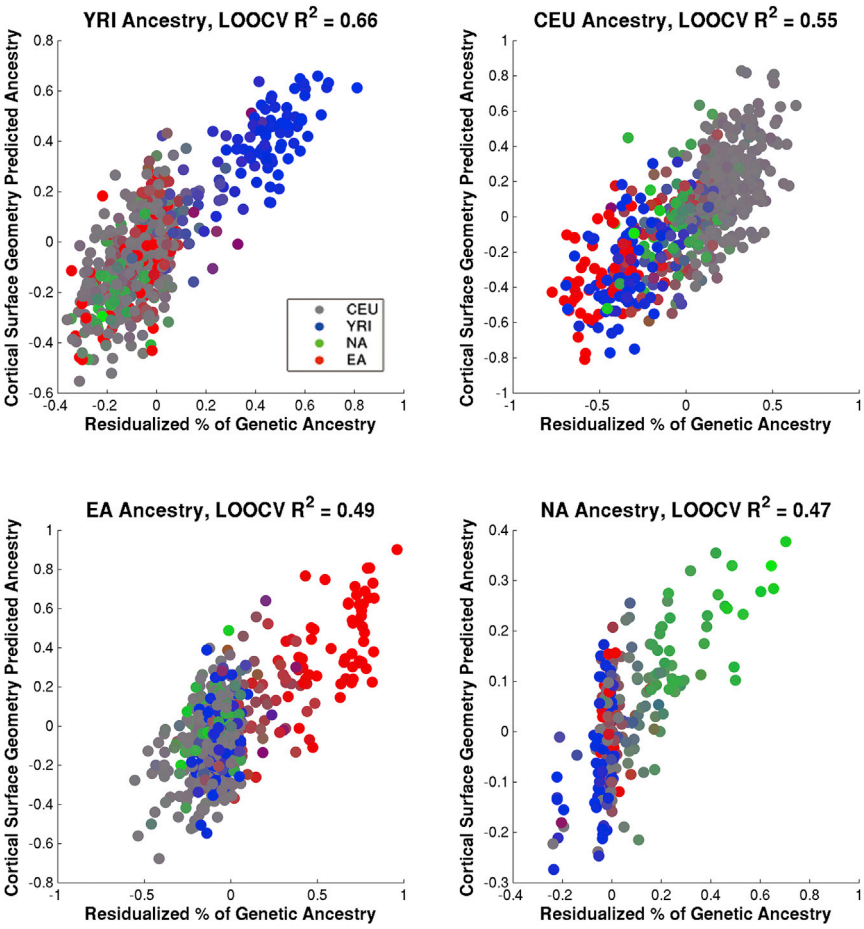

Figure 1. Predicting the Proportion of Genetic Ancestry by Cortical Surface Geometry

YRI: Yoruban, as a proxy for West African ancestry; CEU: Utah residents with Northern and Western European ancestry; EA: East Asian; NA: Native American. In all predictive models, the variables have been residualized with respect to age, age squared, gender, total brain volumes, and scanner used. All models excluded individuals with a 0% proportion of genetic ancestry to that specific component. The colors of the data points are determined by the proportion of genetic ancestry as illustrated in the key in the upper left panel. LOOCV: leave-one-out cross-validation.

the cortical surfaces from all individuals' T1-weighted scans and then represented the positions of the corresponding surface vertices using standard 3D Cartesian coordinates. The reconstruction and registration processes ensure that each vertex on the reconstructed cortical surface is located in a homologous position with respect to the curvature patterns for individuals [15, 16]. Taking the coordinates of all vertices as a whole, we then have information about shape variation of the cortical surface, including aspect ratios, sulcal depth, and gyrification. The prediction models were fit with ridge regression while treating gender, age, age squared, total brain volumes, and the scanner on which the image data were acquired as nuisance covariates. The model performance was evaluated using leave-one-out cross-validation (LOOCV).

As Figure 1 shows, the geometry of the cortical surface has good predictive value for each of the ancestry components. The variances explained by the models are 66% for ancestry in YRI, 55% for ancestry in CEU, 49% for ancestry in EA, and 47% for ancestry in NA. To determine to what degree the geometric differences reflect variation in area expansion of cortical surface, comparable models were computed using vertex-wise surface area (Table 1). Also, to examine possible roles in the prediction of simpler morphological attributes, such as aspect ratios of the cerebrum and volumes of subcortical structures, we conducted comparable analyses predicting ancestry from these measures. None had as much information about ancestry as the geometry of cortical surface did (Table 1).

Characterization of the Cortical Shape Morphs

We then reconstructed the 3D geometry of the cortical surface based on the linear relationship we observed between cortical surface geometry and proportion of genetic ancestry. This allowed us to visualize how the geometry of the cortical surface changes as a function of increasing proportion of genetic ancestry in each ancestral component. The morphing of 3D cortical surfaces from neutral ancestry (25% of genetic ancestry in all four components) to 100% ancestry in each component is demonstrated in Figure 2 (for dynamic morphing of surface geometry, see Movies S1, S2, S3, and S4). As Figure 2 illustrates, the textural contrasts between regions of the cortical surface indicate that the morphing process has complex, unique patterns for each ancestral component, while the intensity varies from region to region. For example, as the proportion of the YRI component increases, the temporal surfaces move posteriorly and inward. The proportion of the CEU component is associated with protrusion of the occipital and frontal surfaces. Increases in the proportion of the EA component are accompanied by variations in temporal-parietal regions. The NA component is associated with flattening of the frontal and occipital surfaces.

Figure 3 summarizes the mean magnitudes and variations of the morphing in each cortical surface region defined by genetic correlations [17]. The mean magnitudes vary from cortical region to cortical region, corresponding to the description above. In addition, YRI, EA, and NA all have relatively high magnitude and variations of morphing in the posterolateral-temporal region.

DISCUSSION

Our data indicate that the unique folding patterns of gyri and sulci are closely aligned with genetic ancestry. The geometry robustly predicts each individual's genetic background even though the population has been shaped by waves of migration and admixtures [12, 18]. A previous study, using only facial

Table 1. Percentage of Variance Explained in Different Predictive Models

	Cortical Surface Geometry	Cortical Surface Area	Brain Aspect Ratios	Subcortical Volumes
YRI	66%	17%	10%	5%
CEU	55%	12%	2%	2%
EA	49%	9%	6%	6%
NA	47%	9%	9%	0%

Cortical surface geometry and cortical surface area were sampled in icosahedral level 4, which contains 642 vertices in each hemisphere. All models were fit with the same setting and evaluated with leave-one-out cross-validation (LOOCV). Nuisance covariates gender, age, age squared, total brain volumes, and scanner were regressed out before calculating the variance explained in LOOCV.

features, achieved 64% explained variance in YRI ancestry among African Americans [19]. Our 3D representation of cortical surface geometry performs similarly in predicting YRI ancestry and also performs well for the other three continental ancestries. As data in Table 1 show, the explanatory power is not due to the differences in total brain volumes, nor to the differences in areal expansion of the cortical surface. Instead, regional folding patterns characterize each ancestral lineage.

On the other hand, the global shapes of the reconstructed cortical surface geometry match W.W. Howells' description of craniometry of 2,524 ancient human crania from 28 populations [20]. Crania of African ancestry tended to have a narrower cranial base, and those of Northern European ancestry had elongated occipital and frontal regions. Crania of East Asian ancestry had a high cranial vault, and crania of Native American ancestry were flatter. Regarding the morphing differences of YRI, EA, and NA, all had high magnitude and variations in the posterior-temporal regions (Figure 3).These findings are consistent with the notion that temporal bones contain more variations across ancestral groups [6].

At first glance, these results are surprising because our model is based on the contemporary United States population, which is the historical product of migrations, slave trades, and local admixture events [18, 21, 22]. Nevertheless, the coordinates of reference-inferred PC space reflect information about individuals' ancestral origins (Figure S1) [14, 21, 23]. Our group's previous study also showed that individuals' positions in PC space are matched with their ancestral locations, rather than their current geographic locations [9]. Therefore, our 3D representation might to a certain degree reflect the neuroanatomical and/or neurocranial changes along the human migratory path in the dispersal from Africa [24]. Based on our current model, we simulated what might be expected from the "out of Africa" scenario in the Supplemental Experimental Procedures (Figure S3; Movie S5).

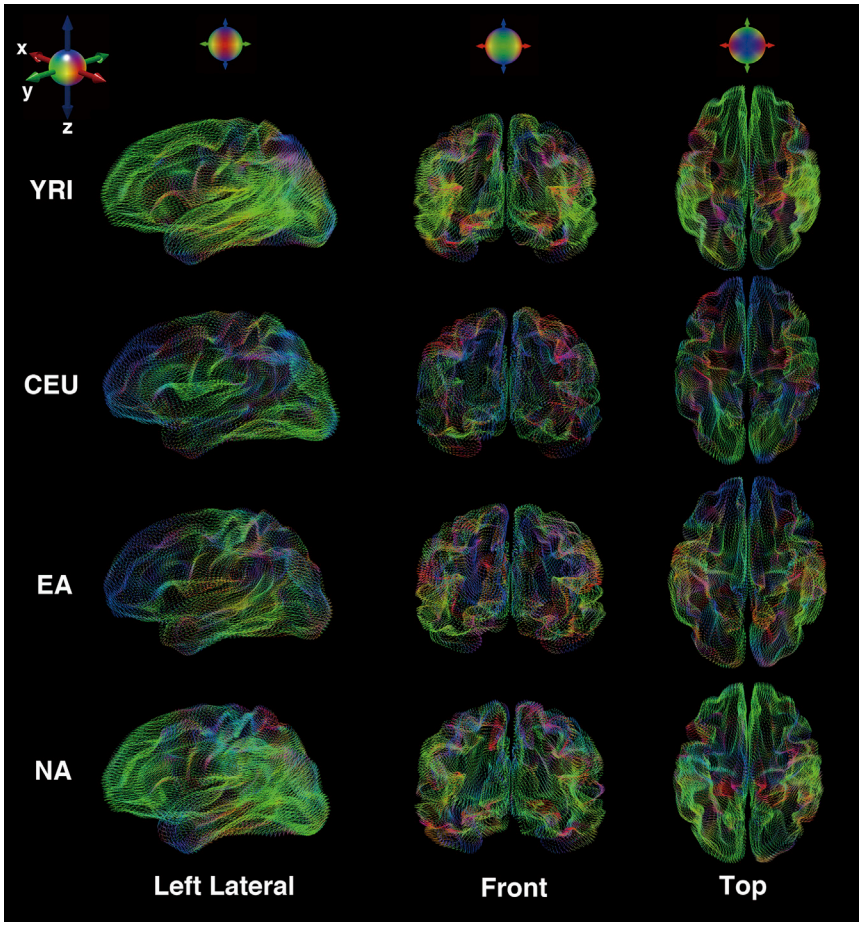

Figure 2. Color-Coded Morphing Process of the 3D Geometry of the Cortical Surface

The still image illustrates how each vertex on the cortical surface morphs from an ancestry-neutral 3D cortical surface (a 25% proportion of genetic ancestry in all ancestral components) to a 3D cortical surface with a 100% proportion of genetic ancestry in a specific ancestral component. The morphing coefficients were estimated from the PING sample. Here, the colors represent the direction of the morphing process. Movement along the medial-lateral axis is coded in red, along the anterior-posterior axis in green, and along the dorsal-ventral axis in blue. The final color is the combination of these three, depending on which direction the vertices move. For each viewing perspective, the coloring frame of reference is rendered on the top of each column. The length of each morphing line is the actual distance between two 3D cortical surfaces. For dynamic morphing animations, see Movies S1, S2, and S3.

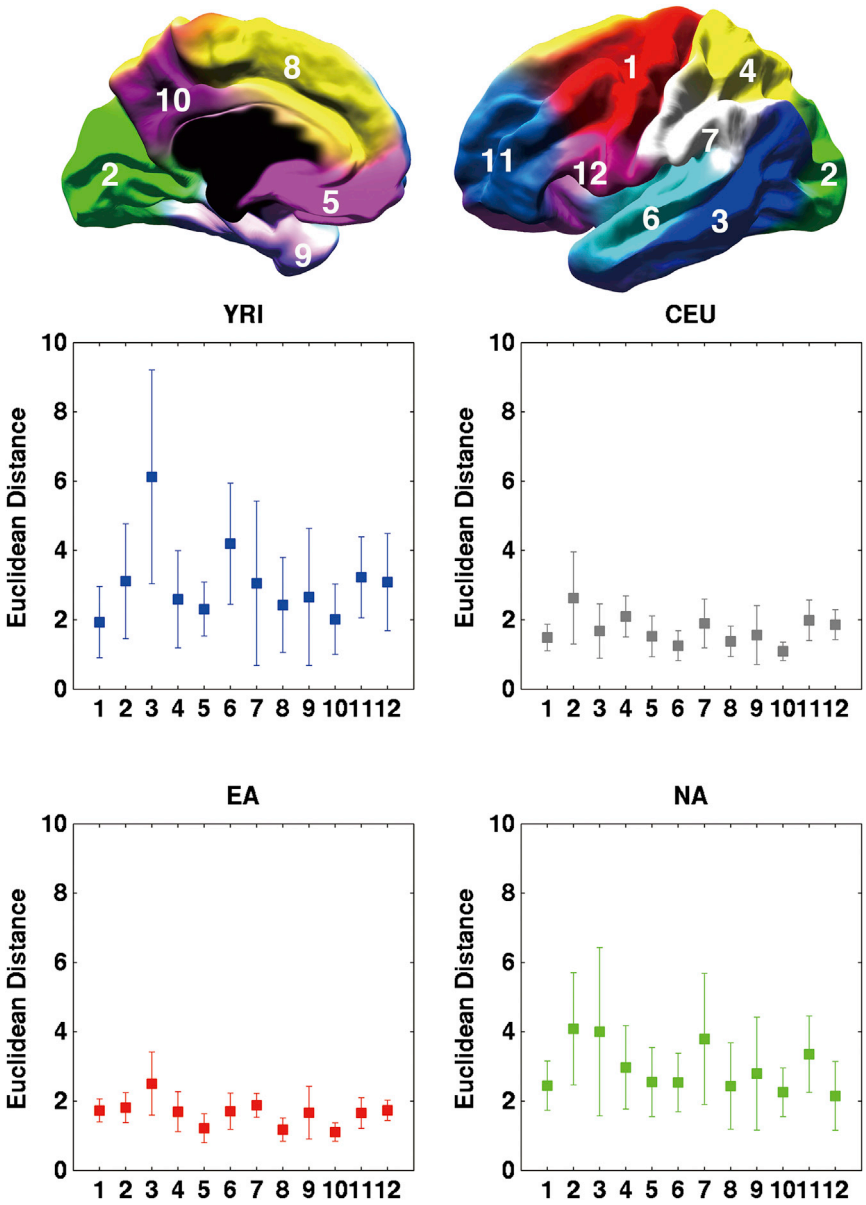

Figure 3. Mean Magnitude and Variations of Morphing across Twelve Regions of Cortical Surface

The following regions are labeled at the top, as defined in a previous publication [17]: 1, central region; 2, occipital cortex; 3, posterolateral temporal region; 4, superior parietal region; 5, orbitofrontal region; 6, superior temporal region; 7, inferior parietal region; 8, dorsomedial frontal region; 9, anteromedial temporal region; 10, precuneus;11, dorsolateral prefrontal cortex; 12, pars opercularis. The Euclidean distances between cortical surface of 100% ancestry and neutral ancestry were calculated for each vertex. The mean and standard deviations of the Euclidean distances for different cortical regions are shown in the bar plots.

More precise characterization of an individual's ancestral origins would require more complex estimates of ancestry based on global-scale reference panels [25]. Further understanding of neuroanatomical change associated with the ''out of Africa'' scenario based on brain imaging data will require future studies using sampling methods similar to those of the Human Genome Diversity Project [26].

It is important to note that these ancestry-related geometric features of the cortical surface are not substantially attributable to variation in cortical surface area. Previous studies of ancient crania often interpreted the shape differences as evidence of relative size alterations of different cortical functional domains [5, 27]. Our results suggest that in the case of the contemporary United States population, the differences in cortical surface geometry might not reflect variation in the relative surface area of different functional cortical regions. In prior studies, regionalization of the cortex was linked to cognitive differences in humans [3, 4]. Any functional significance of the cortical surface geometry per se remains to be established. The effects reported here might be mediated by neutral drift of the phenotypic variations [28]. They could also result from a complex interaction between the brain and neurocranium, with the former expanding while the latter acts as physical resistance. Nevertheless, the causal relationships between the observed shapes and crania are beyond the scope of our current study.

An implication of our ancestry-related 3D models is that, unless properly controlled for, hidden population structures could present a challenge in brain imaging studies of admixed populations [23]. The regional differences between ancestral groups include changing sulcus depths and folding angles. This issue becomes particularly relevant in large, multisite United States and international brain imaging studies [29]. With the advent of inexpensive high-throughput genotyping, it is now possible to control for spurious ancestry admixture effects by using genetically derived admixture factors in the statistical analysis of data [3, 4]. It is also possible that the phenomena we observed are linked with specific ancestral haplotypes. It may therefore be possible to use the ancestral information to improve statistical power for gene discovery with methods such as admixture mapping [30].

SUPPLEMENTAL INFORMATION

Supplemental Information includes three figures, one table, Supplemental Experimental Procedures, and five movies and can be found with this article online at http://dx.doi.org/10.1016/j.cub.2015.06.006.

ACKNOWLEDGMENTS

All data used in this article were obtained from the Pediatric Imaging, Neurocognition, and Genetics (PING) database (http://pingstudy.ucsd.edu). The

investigators within PING contributed to the design and implementation of PING but did not necessarily participate in this study. Data collection and sharing for this project were funded by PING (NIH grant RC2DA029475). Funding was provided by the National Institute on Drug Abuse and the Eunice Kennedy Shriver National Institute of Child Health and Human Development. PING data are disseminated by the PING Coordinating Center at the Center for Human Development, University of California, San Diego. Other support was provided by National Institute of Mental Health grant R01MH100351. A.M.D. is a founder of and holds equity interest in CorTechs Labs and serves on its scientific advisory board. The terms of this arrangement have been reviewed and approved by the University of California, San Diego, in accordance with its Conflict of Interest policies.

Received: March 1, 2015
Revised: May 4, 2015
Accepted: June 1, 2015
Published: July 9, 2015

REFERENCES

1. Falk, D. (2014). Interpreting sulci on hominin endocasts: old hypotheses and new findings. Front. Hum. Neurosci. *8*, 134.
2. Holloway, R.L. (2008). The human brain evolving: a personal retrospective. Front. Neuroanat. *37*, 1–19.
3. Fjell, A.M., Walhovd, K.B., Brown, T.T., Kuperman, J.M., Chung, Y., Hagler, D.J., Jr., Venkatraman, V., Roddey, J.C., Erhart, M., McCabe, C., et al.; Pediatric Imaging, Neurocognition, and Genetics Study (2012). Multimodal imaging of the self-regulating developing brain. Proc. Natl. Acad. Sci. USA *109*, 19620–19625.
4. Walhovd, K.B., Fjell, A.M., Brown, T.T., Kuperman, J.M., Chung, Y., Hagler, D.J., Jr., Roddey, J.C., Erhart, M., McCabe, C., Akshoomoff, N., et al.; Pediatric Imaging, Neurocognition, and Genetics Study (2012). Long-term influence of normal variation in neonatal characteristics on human brain development. Proc. Natl. Acad. Sci. USA *109*, 20089–20094.
5. Bruner, E., de la Cuétara, J.M., Masters, M., Amano, H., and Ogihara, N. (2014). Functional craniology and brain evolution: from paleontology to biomedicine. Front. Neuroanat. *8*, 19.
6. Reyes-Centeno, H., Ghirotto, S., Détroit, F., Grimaud-Hervé, D., Barbujani, G., and Harvati, K. (2014). Genomic and cranial phenotype data support multiple modern human dispersals from Africa and a southern route into Asia. Proc. Natl. Acad. Sci. USA *111*, 7248–7253.
7. Manica, A., Amos, W., Balloux, F., and Hanihara, T. (2007). The effect of ancient population bottlenecks on human phenotypic variation. Nature *448*, 346–348.
8. Lieberman, D.E., McBratney, B.M., and Krovitz, G. (2002). The evolution and development of cranial form in Homosapiens. Proc. Natl. Acad. Sci. USA *99*, 1134–1139.
9. Bakken, T.E., Dale, A.M., and Schork, N.J. (2011). A geographic cline of skull and brain morphology among individuals of European Ancestry. Hum. Hered. *72*, 35–44.
10. Brown, T.T., Kuperman, J.M., Chung, Y., Erhart, M., McCabe, C., Hagler, D.J., Jr., Venkatraman, V.K., Akshoomoff, N., Amaral, D.G., Bloss, C.S., et al. (2012). Neuroanatomical assessment of biological maturity. Curr. Biol. *22*, 1693–1698.
11. Jernigan, T.L., Brown, T.T., Hagler, D.J., Jr., Akshoomoff, N., Bartsch, H., Newman, E., Thompson, W.K., Bloss, C.S., Murray, S.S., Schork, N., et al.; Pediatric Imaging, Neurocognition, and Genetics Study (2015). The Pediatric Imaging, Neurocognition, and Genetics (PING) Data Repository. Neuroimage. Published online May 1, 2015. http://dx.doi.org/10.1016/j.neuroimage.2015.04.057.
12. Reich, D., Patterson, N., Campbell, D., Tandon, A., Mazieres, S., Ray, N., Parra, M.V., Rojas, W., Duque, C., Mesa, N., et al. (2012). Reconstructing Native American population history. Nature *488*, 370–374.
13. Altshuler, D.M., Gibbs, R.A., Peltonen, L., Altshuler, D.M., Gibbs, R.A., Peltonen, L., Dermitzakis, E., Schaffner, S.F., Yu, F., Peltonen, L., et al.; International HapMap 3 Consortium (2010). Integrating common and rare genetic variation in diverse human populations. Nature *467*, 52–58.
14. Chen, C.Y., Pollack, S., Hunter, D.J., Hirschhorn, J.N., Kraft, P., and Price, A.L. (2013). Improved ancestry inference using weights from external reference panels. Bioinformatics *29*, 1399–1406.
15. Fischl, B., Sereno, M.I., and Dale, A.M. (1999). Cortical surface-based analysis. II: Inflation, flattening, and a surface-based coordinate system. Neuroimage *9*, 195–207.
16. Dale, A.M., Fischl, B., and Sereno, M.I. (1999). Cortical surface-based analysis. I. Segmentation and surface reconstruction. Neuroimage *9*, 179–194.
17. Chen, C.H., Gutierrez, E.D., Thompson, W., Panizzon, M.S., Jernigan, T.L., Eyler, L.T., Fennema-Notestine, C., Jak, A.J., Neale, M.C., Franz, C.E., et al. (2012). Hierarchical genetic organization of human cortical surface area. Science *335*, 1634–1636.
18. Tishkoff, S.A., Reed, F.A., Friedlaender, F.R., Ehret, C., Ranciaro, A., Froment, A., Hirbo, J.B., Awomoyi, A.A., Bodo, J.M., Doumbo, O., et al. (2009). The genetic structure and history of Africans and African Americans. Science *324*, 1035–1044.
19. Claes, P., Liberton, D.K., Daniels, K., Rosana, K.M., Quillen, E.E., Pearson, L.N., McEvoy, B., Bauchet, M., Zaidi, A.A., Yao, W., et al. (2014). Modeling 3D facial shape from DNA. PLoS Genet. *10*, e1004224.
20. Howells, W.W. (1989). Skull Shape and the Map: Craniometric Analyses in the Dispersion of Modern *Homo*. (Harvard University Press), pp. 63–64.
21. Li, J.Z., Absher, D.M., Tang, H., Southwick, A.M., Casto, A.M., Ramachandran, S., Cann, H.M., Barsh, G.S., Feldman, M., Cavalli-Sforza, L.L., and Myers, R.M. (2008). Worldwide human relationships inferred from genome-wide patterns of variation. Science *319*, 1100–1104.
22. Abdulla, M.A., Ahmed, I., Assawamakin, A., Bhak, J., Brahmachari, S.K., Calacal, G.C., Chaurasia, A., Chen, C.H., Chen, J., Chen, Y.T., et al.; HUGO Pan-Asian SNP Consortium; Indian Genome Variation Consortium (2009). Mapping human genetic diversity in Asia. Science *326*, 1541–1545.
23. Price, A.L., Patterson, N.J., Plenge, R.M., Weinblatt, M.E., Shadick, N.A., and Reich, D. (2006). Principal components analysis corrects for stratification in genome-wide association studies. Nat. Genet. *38*, 904–909.
24. Cavalli-Sforza, L.L., Menozzi, P., and Piazza, A. (1993). Demic expansions and human evolution. Science *259*, 639–646.
25. Yang, W.Y., Novembre, J., Eskin, E., and Halperin, E. (2012). A model-based approach for analysis of spatial structure in genetic data. Nat. Genet. *44*, 725–731.
26. Cavalli-Sforza, L.L. (2005). The Human Genome Diversity Project: past, present and future. Nat. Rev. Genet. *6*, 333–340.
27. Bruner, E., Manzi, G., and Arsuaga, J.L. (2003). Encephalization and allometric trajectories in the genus Homo: evidence from the Neandertal and modern lineages. Proc. Natl. Acad. Sci. USA *100*, 15335–15340.
28. Roseman, C.C. (2004). Detecting interregionally diversifying natural selection on modern human cranial form by using matched molecular and morphometric data. Proc. Natl. Acad. Sci. USA *101*, 12824–12829.
29. Medland, S.E., Jahanshad, N., Neale, B.M., and Thompson, P.M. (2014). Whole-genome analyses of whole-brain data: working within an expanded search space. Nat. Neurosci. *17*, 791–800.
30. Winkler, C.A., Nelson, G.W., and Smith, M.W. (2010). Admixture mapping comes of age. Annu. Rev. Genomics Hum. Genet. *11*, 65–89.

